THE ASTROPHYSICAL JOURNAL, 408:586–592, 1993 May 10

PHOTOMETRY AND IMAGING OF THE PECULIAR PLANETARY NEBULA IRAS 21282+5050

SUN KWOK,[1,2] BRUCE J. HRIVNAK,[1,3,4] AND PHILIP P. LANGILL[1,2]

Received 1992 August 3; accepted 1992 November 4

ABSTRACT

We report visible, near-infrared, and mid-infrared photometry of the *IRAS* planetary nebula 21282+5050. Narrow-band photometry at 10 μm confirms the presence of the 11.3 μm PAH feature. IRAS 21282+5050 belongs to a small group of planetary nebulae with WC11 nuclei and PAH emission. The spectral energy distribution shows that majority of the flux is emitted in the infrared, and the object has one of the highest infrared excesses among all planetary nebulae. Optical imaging (after subtraction of the central star) reveals a nebula of size of $\sim 7'' \times 5''$ which is elongated along the N-S direction.

Subject headings: infrared: interstellar: continuum — planetary nebulae: individual (IRAS 21282+5050)

1. INTRODUCTION

IRAS 21282+5050 belongs to a class of cool *IRAS* sources which show the 7.7, 8.6, and 11.3 μm emission features in their *IRAS* low-resolution spectra (LRS) (Cohen, Tielens, & Allamandola 1985; de Muizon et al. 1986). These features are part of a family of infrared features (3.3, 3.4, 6.2, 7.7, 8.6, and 11.3 μm) that are commonly observed in objects with ionization fronts (Willner 1984), such as planetary nebulae, reflection nebulae, H II regions, and some extragalactic objects. Optical spectroscopy by Cohen & Jones (1987) has identified 21282+5050 as a planetary nebula with an 07(f)–WC11 nucleus. Circumstellar molecular CO emission has also been detected (Huggins & Healy 1989; Likkel et al. 1988, 1991; Volk, Kwok, & Woodsworth 1992), suggesting that it is a young planetary nebula.

IRAS 21282+5050 is unusual is several ways. Its optical brightness ($V = 14.4$ in the continuum) is weak in comparison to its brightness in the far-infrared. While many young planetary nebulae have strong infrared excesses, it is rare for the infrared flux to contribute more than half of the total emergent flux (Zhang & Kwok 1991). IRAS 21282+5050 is also a member of a small class (six members at present) of low-excitation planetary nebulae with similar WC11 central stars (Menzies & Wolstencroft 1990; Zijlstra et al. 1991; Hu & Bibo 1990). In the 3 μm region, in addition to the well-known features at 3.29 and 3.40 μm, IRAS 21282+5050 also shows features at 3.46, 3.52, and possibly 3.56 μm (de Muizon et al. 1986; Nagata et al. 1988). These have been seen in only one other planetary nebula, NGC 7027 (Nagata et al. 1988), and in several H II regions (Jourdain de Muizon et al. 1990b). The features at 7.7, 8.6, and 11.3 μm are strong in its LRS spectrum (Volk & Cohen 1990). In common with NGC 7027, IRAS 21282+5050 possesses a flux ratio of the 8.6 to the 11.3 μm feature of less than 1.0, an emission plateau from 11 to 13 μm, and perhaps some additional weak features in this latter wavelength interval (Roche, Aitken, & Smith 1991; Witteborn et al. 1989).

As part of our program to determine the energy distributions of cool *IRAS* sources, we have obtained ground-based observations of IRAS 21282+5050 from 0.45 to 20 μm. We have also obtained high-resolution images in an attempt to resolve the object in the visible.

2. OBSERVATIONS

We observed IRAS 21282+5050 in the near-infrared on 1989 August 17 on Mauna Kea with the UKIRT 3.8 m telescope in the f/35.4 configuration. The InSb photometer (UKT9) was used with *J*, *H*, *K*, *L'*, and a narrow *M* filters. The beam profiles was found to be 7".8 in decl. × 8".3 in R.A. by scanning the B5 IV star τ Her. A 20" chop at 3.5 Hz was employed. Standard stars were observed throughout the night as part of a larger program, giving extinction and zero points in each filter to standardize the observations. The photometry results are listed in Table 1. Mid-infrared observations were obtained on 1989 November 1 at UKIRT through the service observing program. The Ge:Ga bolometer (UKT8) was used with an aperture of 6". Observations were made through five intermediate-band filters, 8.75–12.5 μm, and the broad-band *N* and *Q* filters. Standard stars were observed to determine the nightly extinction coefficients and zero-points, and these were used to transform to standard magnitudes. These results are listed in Table 1. We determined the position of the source to be R.A. = $21^h28^m15^s.5$, decl. = 50°50'47" (1950), with an uncertainty of 2".

Visible photometry was kindly obtained for us by H. C. Harris on 1989 October 1 with the 1.0 m telescope of the United States Naval Observatory (USNO) at Flagstaff, AZ. The observations were made with a CCD and transformed through observations of standard stars to closely match the standard *B*, *V*, I_c system. These are also listed in Table 1. The synthesized continuum magnitudes derived by Cohen & Jones (1987) from their low-resolution spectra are in general agreement with these measurements.

The *IRAS* LRS spectrum of IRAS 21282+5050 was extracted from the *IRAS* LRS data base at the University of Calgary IRAS Data Analysis Facility. A linear baseline has been subtracted from each band, and the two bands were joined together by shifting one band relative to the other. The

[1] Visiting Astronomer at the Canada-France-Hawaii Telescope, operated by the National Research Council of Canada, the Centre National de Recherche Scientifique of France, and the University of Hawaii.

[2] Postal address: Department of Physics and Astronomy, The University of Calgary, Calgary, Alberta, Canada T2N 1N4.

[3] Department of Physics and Astronomy, Valparaiso University, Valparaiso, IN 46383.

[4] Dominion Astrophysical Observatory, National Council of Canada, 5071 W. Saanich Road, Victoria, B.C., Canada V8X 4M6.

TABLE 1

GROUND-BASED PHOTOMETRY OF 21282+5050

A. VISIBLE

B	V	I_c
15.75	14.31	12.57

B. NEAR-INFRARED

J	H	K	L′	M
11.53	10.75	9.51	6.59	5.80

C. MID-INFRARED

8.75 μm	9.6 μm	10.3 μm	11.6 μm	12.5 μm	N	Q
0.73	0.76	0.41	−0.75	−0.98	−0.03	−1.83

NOTE.—Observational uncertainties (in mag) are as follows: visible: 0.02; near-infrared: 0.03 (*J*, *H*), 0.02, (*K*, *L*′), 0.04 (*M*); mid-infrared: 0.02 (narrow bands, *N*), 0.03 (*Q*).

flux values have been recalibrated using the LRS correction factors of Volk & Cohen (1989).

In Figure 1 we have plotted the energy distribution of IRAS 21282+5050 based upon the new observations listed in Table 1, the four *IRAS* photometry points (corrected for color), and the *IRAS* LRS. The LRS spectrum was made to agree with the *IRAS* 12 μm flux by convolving it with the instrumental profile of the 12 μm band and normalized to the 12 μm in-band flux. The LRS spectrum is in good agreement with the UKIRT intermediate-band measurements, confirming the presence of the PAH features.

Optical imaging was carried out on 1990 August 27 on the 3.6 m Canada-France-Hawaii Telescope (CFHT) using the DAO/CFHT image-stabilizing High Resolution Camera (HRCam). Details of the camera design are given by McClure et al. (1989). A SAIC 102 × 1024 CCD was used as the detector, with each pixel corresponding to 0″.13 on the sky. The filters used were *V* and *I* ("Mould") filters and an intermediate-band 5007 Å ($\Delta\lambda \sim 100$ Å) filter. Two exposures were made in each filter, and the exposures were co-added to give a single image in each band. Since the [O III] λ5007 emission is weak from the object (see Cohen & Jones 1987), this band basically is recording the continuum light. Due to thin cirrus, the sky conditions were not photometric, and the seeing varied during these observations. The images were reduced-biased subtracted and flat-fielded using IRAF. By examining field stars on these frames we determined the resolution (FWHM) to be 0″.61, 0″.84, and 0″.78 in 5007 Å, *V*, and *I* respectively.

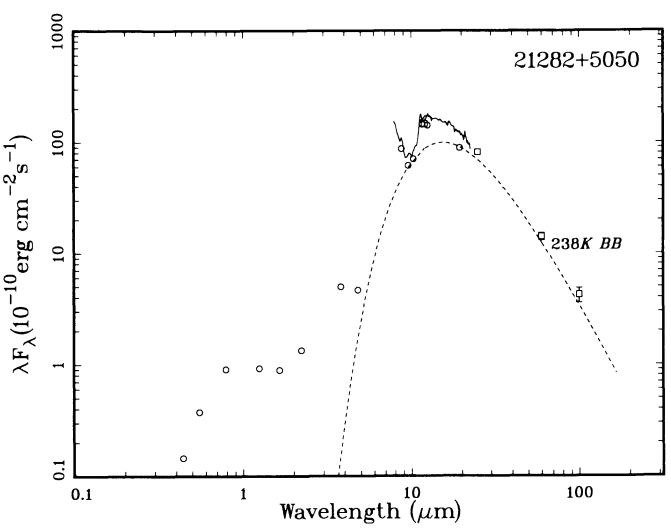

FIG. 1.—Energy distribution of IRAS 21282+5050. The open squares are color-corrected *IRAS* broad-band fluxes. The solid line between 7 and 23 μm is the *IRAS* LRS spectrum. Also plotted in dashed line is a 238 K blackbody curve as an approximation to the dust component.

The 5007 Å image is shown in Figure 2. North is up and east is to the left. The outer contours are drawn at 3 σ_{sky} above the surrounding sky brightness. The standard deviation of the sky counts, σ_{sky}, was found by sampling ten 5 × 5 pixel areas or 0″.65 × 0″.65, approximately that of the seeing profile. The inner contours are drawn at the 10, 20, 30, and 40 σ_{sky} level. The brightness of IRAS 21282+5050 is indicated by the innermost contour (1600 σ). In Figure 2*a* we display the total image of the object and a field star.

We then show the effects of removing the light of the star from the image. This was investigated using the stellar profile-fitting program DAOPHOT (Stetson 1987). An average point-spread function (PSF) was determined from over 30 field stars in the image. How well this PSF matches the stars in the field was tested by scaling it to the peak brightness of a field star and subtracting it from the star. This did a very good job of removing the stars from the entire field. We found that scaling the PSF to the peak brightness of IRAS 21282+5050 before subtraction resulted in the appearance of a "hole" in the brightness contours extending east of the stellar position. This "hole" results from attributing 100% of the peak brightness to the star and 0% to the nebula. Since undoubtedly some flux comes from the nebula, we have experimented with attributing various amounts of the peak brightness to the nebula and subtracting the remainder as due to the star, and also with slightly shifting the stellar position away from the position of peak brightness. We find that the "hole" can be removed either by attributing 3.5% of the peak brightness to the nebula, or by a shift of 0.02 pixels westward in the assumed position of the star and attributing 2.5% of the peak brightness to the nebula. Figure 2*b* shows the circumstellar nebula of IRAS 21282+5050 resulting from the first of these two cases.

The nebula appears to be asymmetric and is extended in the N-S direction (with a slight tilt to the northeast) with a size of 6″.5 × 4″.8. The values attributed above to the contribution of the nebula to the central peak were chosen by trial and error to remove the central "hole" in the brightness contours. They are arbitrary, but seem reasonable. Even if we attribute 5%, 10%, or even 20% of the peak light to the nebula, the outer contours remain the same. The nebula has a similar appearance in the *V*- and *I*-band images.

Note also that the central part of the nebula shows double brightness peaks along the direction of the major axis of the outer structure. "Double-peaked" structures are also common in the radio images of compact planetary nebulae (Aaquist & Kwok 1990, 1991) and are probably due to projection effects of incomplete shells formed under the interacting winds mechanism with an asymmetric AGB wind (Volk & Leahy 1993).

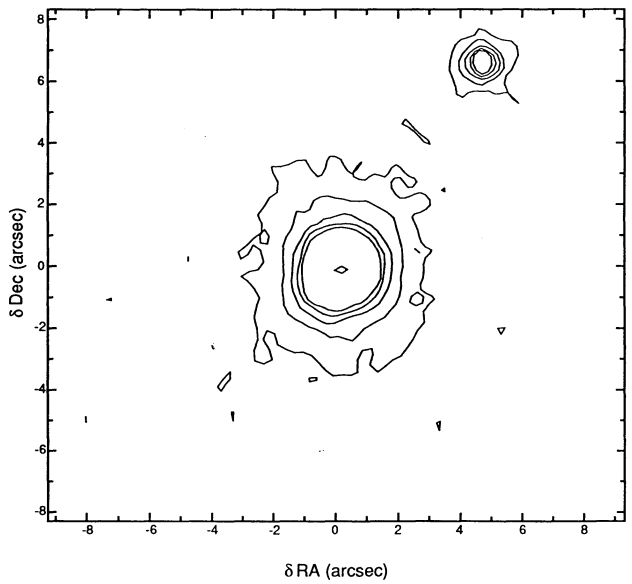

FIG. 2a

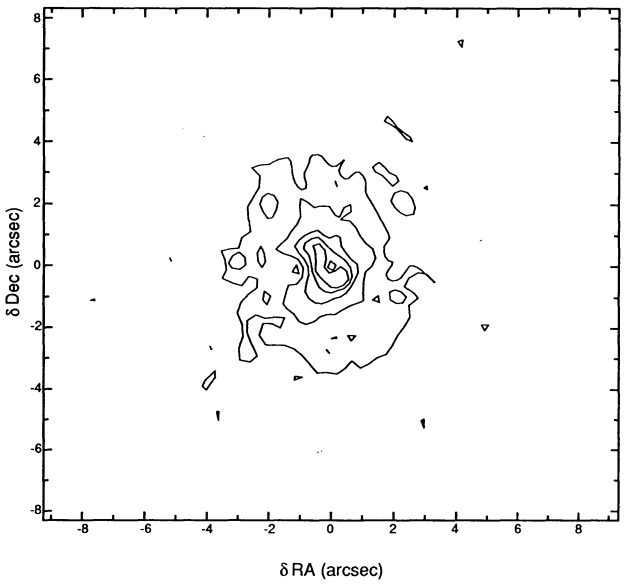

FIG. 2b

FIG. 2.—Contour plots of the [5007 Å] image of IRAS 21282+5050. The outer contour is at the 3 σ_{sky} level, and the inner contours are at 10, 20, 30, and 40 σ_{sky}. The position of peak brightness is indicated by the innermost contour. The resolution in the image is 0".61. The direction of north is up and east to the left. (*a*) The total [5007 Å] image of 21282+5050 (star plus nebula). The innermost contour is at 1600 σ. (*b*) The image after star subtraction, with 3.5% of the peak brightness of 21282+5050 attributed to the nebula and the remainder to the star. Note that the field star on the upper-right corner disappears after subtraction.

However, the optical image is due to scattering, whereas the radio (and mid-infrared) images are due to emission, and there is no reason to believe that the optical and radio morphologies are related.

3. DISCUSSION

3.1. *The Evolutionary Status of* IRAS 21282+5050

We can see from Figure 1 that most of the observed flux in IRAS 21282+5050 is from the dust component. The dust continuum can be reasonably approximated by a blackbody of 283 K. Although the dust emission from most planetary nebulae corresponds to single-temperature blackbodies, the color temperatures of the nebulae are almost always less than 200 K, even for the youngest nebulae (Zhang & Kwok 1991). Since the dust component represents the remnant of the AGB circumstellar envelope, its temperature is expected to decrease as the nebula expands. The dust temperature of planetary nebulae therefore is inversely related to the time since the star has left the asymptotic giant branch (Kwok 1990). Comparison of the high dust temperature in IRAS 21282+5050 with the evolutionary models of Volk (1992) suggests that IRAS 21282+5050 left the AGB only a short time ($<10^3$ yr) ago.

The strong infrared excess in IRAS 21282+5050 suggests that the optical nebula is heavily obscured by circumstellar dust. By comparing the spectrum of IRAS 21282+5050 with that of an 07(f) star, Cohen & Jones (1987) derived an extinction (A_v) of 5.7 mag. Due to the position in the plane of the Galaxy ($l = 94°$, $b = 0°$), the visible light from IRAS 21282+5050 suffers a large amount of interstellar extinction. Based on the reddening studies of FitzGerald (1968) and Neckel & Klare (1980), one would expect interstellar extinction of approximately 2.5 mag, for a distance of 1–3 kpc. This implies circumstellar extinction of 3.2 mag. Even after correcting for 2.5 mag of interstellar extinction (which will raise the flux at V by a factor of 10), the emission in the visible is still much weaker than the level of the observed dust component emission. Comparing the energy distribution corrected for interstellar extinction with the energy distribution of young planetary nebulae in Zhang & Kwok (1991), we again come to the conclusion that this nebula is younger (in dynamical age) than almost all planetary nebulae known to date.

The facts that IRAS 21282+5050 has one of the highest infrared excesses observed in a planetary nebula, and that the central star has evolved to a high enough temperature to ionize the circumstellar nebula suggest that it must have evolved very quickly from the AGB. Comparison with the evolutionary tracks of Schönberner suggests a central star mass of >0.6 $M_\odot$. In this respect, it is similar to NGC 7027, which has a large infrared excess and a very hot central star (170,000 K). Both objects have extended molecular envelopes, which is another indication of their young age. In more evolved nebulae, the molecular envelopes are expected to be dissociated by the UV radiation from the central star. If we combine our observed angular radius of 3" with the CO expansion velocity of 16 km s^{-1}, we obtain a kinematic age of 900 (D kpc^{-1}) yr. Since the nebular expansion velocity is likely to be higher than the CO expansion velocity, the actual age is probably smaller.

3.2. *Other Planetary Nebulae with WC Nuclei*

IRAS 21282+5050 is one of several planetary nebulae with a [WC11] nucleus and large infrared excess. These are listed together in Table 2, where we have also listed NGC 7027 for comparison. Although the central star of NGC 7027 is much hotter than these others, it shares common properties with the others in the fact that they all show PAH emission features and have large infrared excesses.

Figure 3 shows the LRS spectra for five of the candidates. IRAS 17514−1555 has five scans in the LRS database, but none of them has a good enough signal-to-noise ratio to be

TABLE 2

PLANETARY NEBULAE WITH WC11 NUCLEI AND LARGE INFRARED EXCESSES

IRAS	Other Name	Spectral Type	IR features (μm)	Molecules
04215+6000.....	M4 – 18	WC11[a,b]	8.6,[c] 11.3[c]	...
07027–7934.....	Vo 1[d]	WC11[e]	7.7,[f] 11.3[g]	CO,[h] OH[j]
14562–5406.....	He2 – 113	WC11[b]	3,3,[k] 7.7,[g] 8.6,[l] 11.3[l]	...
17047–5650.....	CPD – 56°8032	WC11[a,b]	3.3,[k] 7.7,[m] 11.3[l]	CO[h]
17514–1555.....	...	WC11[n]	...	...
21282+5050.....	...	WC11[o]	3.3,[p] 7.7,[p] 8.6,[p,q] 11.3[p,q]	CO,[r] HCO^+
	NGC 7027.....	...	3.3, 6.2, 7.7, 8.6, 11.3[s]	CO, CN, HCN, HCO^+, HNC, C_3H_2[t]

[a] Webster & Glass 1974.
[b] Carlson & Henize 1979.
[c] Aitken & Roche 1984.
[d] Volk & Cohen 1990.
[e] Menzies & Wolstencroft 1990.
[f] Jourdain de Muizon et al. 1990.
[g] Cohen et al. 1985.
[h] Loup et al. 1990.
[j] Zijlstra et al. 1991.
[k] Allen et al. 1982.
[l] Aitken et al. 1980.
[m] Cohen et al. 1989.
[n] Hu & Bibo 1990.
[o] Cohen & Jones 1987.
[p] de Muzion et al. 1986.
[q] Roche et al. 1991.
[r] Likkel et al. 1988.
[s] Russell et al. 1977.
[t] Deguchi et al. 1990.

usable. The four brightest sources in Figure 3 are contained in the *IRAS* LRS Atlas (1986), and the two-digit LRS Atlas classification number is given in plot, along with the Volk-Cohen classification of each (Volk & Cohen 1989). The spectrum of M4–18 is poor, with some negative flux values, and the spectrum has been smoothed over three channels. All five spectra have been reprocessed as described above for IRAS 21282+5050.

The 11.3 μm PAH feature can clearly be seen in the four brightest objects (except M4–18) along with the long-wavelength side of the 7.7 μm PAH feature. The 8.6 and 11.3 μm emission features can be seen in ground-based spectropho-

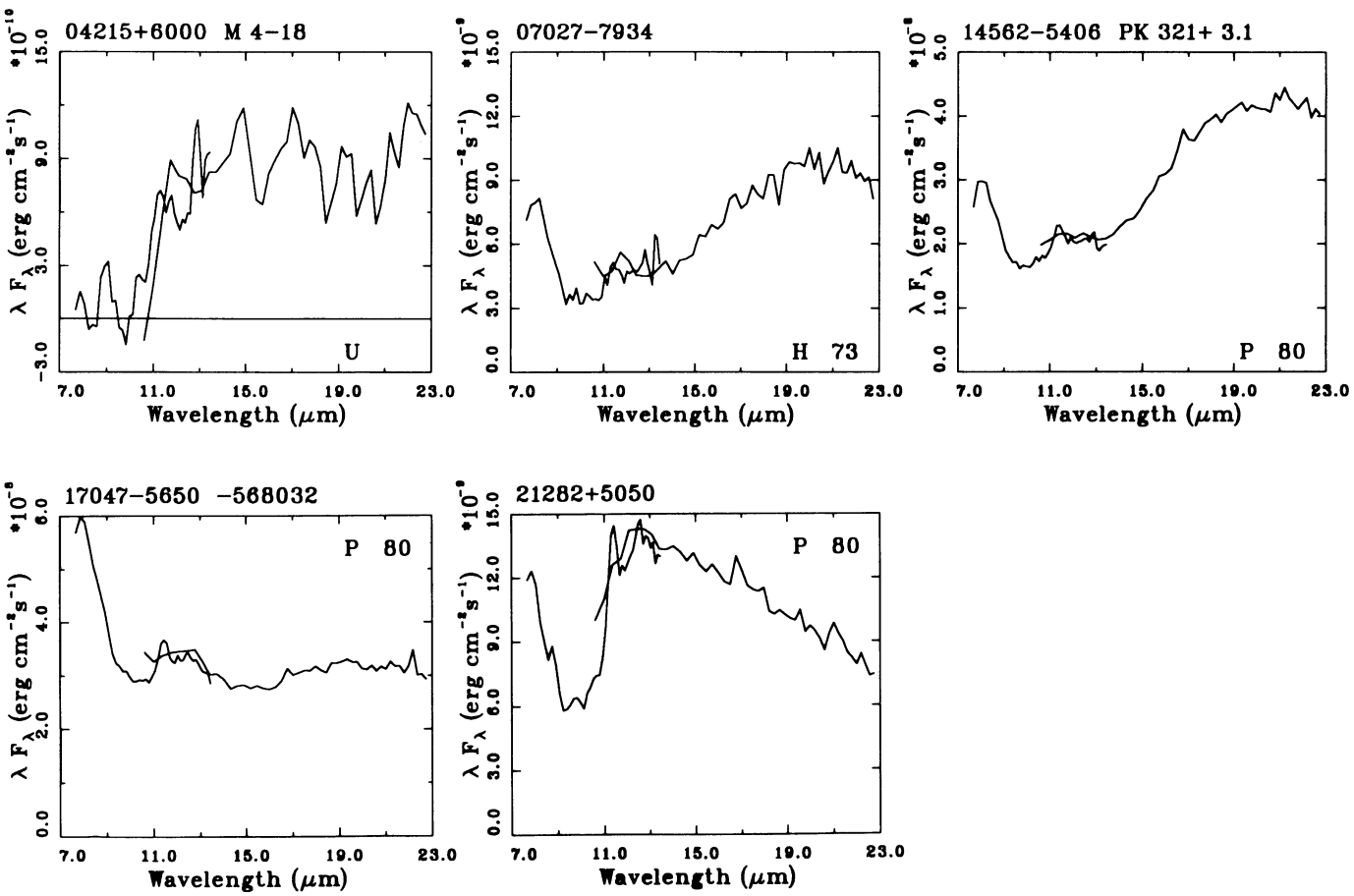

FIG. 3.—*IRAS* LRS spectra for the five of the WC11 objects in Table 2. The two-digit numbers on the right side of the panels are classification codes of the LRS Atlas, and the single character is the classification code as defined by Volk & Cohen (1989).

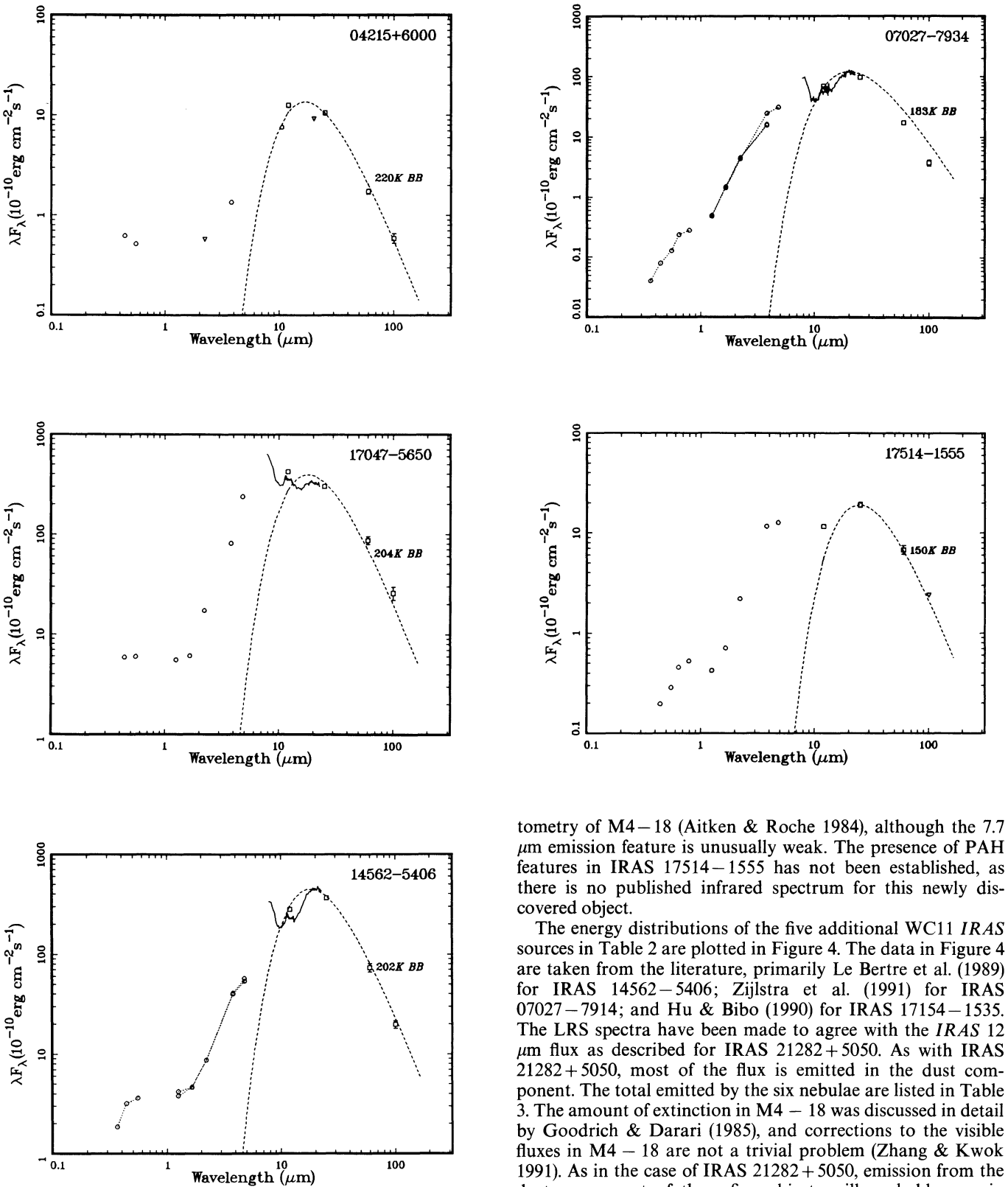

FIG. 4.—Energy distributions of the additional five *IRAS* planetary nebulae with WC11 nuclei. The open squares are color-corrected *IRAS* broadband fluxes, the open circles are ground-based photometry data from the literature, and the solid lines are the *IRAS* LRS spectra. Also shown are blackbody curves (*dashed lines*) as an approximation to the dust components.

tometry of M4−18 (Aitken & Roche 1984), although the 7.7 μm emission feature is unusually weak. The presence of PAH features in IRAS 17514−1555 has not been established, as there is no published infrared spectrum for this newly discovered object.

The energy distributions of the five additional WC11 *IRAS* sources in Table 2 are plotted in Figure 4. The data in Figure 4 are taken from the literature, primarily Le Bertre et al. (1989) for IRAS 14562−5406; Zijlstra et al. (1991) for IRAS 07027−7914; and Hu & Bibo (1990) for IRAS 17154−1535. The LRS spectra have been made to agree with the *IRAS* 12 μm flux as described for IRAS 21282+5050. As with IRAS 21282+5050, most of the flux is emitted in the dust component. The total emitted by the six nebulae are listed in Table 3. The amount of extinction in M4 − 18 was discussed in detail by Goodrich & Darari (1985), and corrections to the visible fluxes in M4 − 18 are not a trivial problem (Zhang & Kwok 1991). As in the case of IRAS 21282+5050, emission from the dust component of these five objects will probably remain dominant even after correction for interstellar extinction.

In the cases of M4−18, Vo-1 and IRAS 17514−1555, in order for their luminosities to be consistent with those of planetary nebulae ($L > 3000\ L_\odot$), they have to be at least 6, 2.5, and

TABLE 3

DERIVED TOTAL FLUXES FROM THE WC11 PLANETARY NEBULAE

IRAS	F_{IR} (ergs cm^{-2} s^{-1})	L/D^2 ($L_\odot$ kpc^{-2})	z/D (pc kpc^{-1})	t/D[a] (yr kpc^{-1})
04215+6000....	2.4 (−9)	0.75 (2)	132	4.2 (2)
07027−7934....	1.6 (−8)	5 (2)	459	1.8 (3)
14562−5406....	6.1 (−8)	19 (2)	70	...
17047−5650....	9.5 (−8)	30 (2)	173	1.5 (2)
17514−1555....	4.2 (−9)	1.3 (2)	86	2.4 (3)
21282+5050....	2.1 (−8)	6.6 (2)	2.1	7.0 (2)

[a] Dynamical age derived from angular size assuming an expansion velocity of 20 km s^{-1}.

5 kpc away, respectively. This will put them at 800, 1000, and 500 pc out of the plane. Such high Galactic latitudes can be avoided if the total fluxes have been severely underestimated. For example, if the dust is heavily concentrated in a disk that lies perpendicular to the plane of the sky and the nebula is ionization bounded in the plane of the disk, then the radiation will be highly extinguished in our direction, and we will be missing significant amounts of photons emitted in the polar directions. However, in order to bring Vo-1 to a z of 150 pc, the total emergent flux would have to be increased by a factor of 50, which is extremely large. Thus there is evidence that some of these WC11 objects were born at high Galactic latitudes and thus presumably have low-mass progenitors.

Nebulae have also been resolved in optical light around Vo-1, with a diameter of 15″ (Zijlstra et al. 1991), and around IRAS 17514−1555, with a diameter of 20″ (Hu & Bibo 1990). Roche, Allen, & Bailey (1986) made speckle observations of CPD−56°8032 at the wavelength of the 3.3 μm emission feature, and found it to be extended with a diameter of 1″.3. We recently imaged CPD−56°8032 in visible light and also found it to be slightly extended. Le Bertre et al. (1989) were unable to resolve He2−113 on CCD images taken through V and Hα filters with an image quality of ∼1″.5. M4−18 was not resolved in the visible (van der Hucht et al. 1981; Goodrich & Dahari 1985), but is found to have a shell structure (diameter 3″.5) typical of planetary nebulae in the radio (angular resolution 0″.4, Aaquist & Kwok 1990).

Using the above angular sizes, the dynamical ages of the nebulae (as a function of distance) can be estimated if one assumes a nebular expansion velocity. These values are listed in Table 3 assuming an expansion velocity of 20 km s^{-1}. Using distances derived from the minimum luminosity of planetary nebulae lends to dynamic ages of a few thousand years, except for 17514−1555, which is somewhat older, and CPD−56°8032, which is much younger. This suggests that CPD−56°8032 has higher luminosity, or is significantly larger than the 3.3 μm size measurement of Roche et al. (1986).

3.3. *Morphology of* IRAS 21282+5050

Likkel et al. (1988) have suggested a size of ∼10″ (FWHM) for the CO-emitting region of IRAS 21282+5050. Using the Nobeyama Millimeter Array with an angular resolution of ∼14″, Shibata et al. (1989) obtained CO(1–0) velocity maps showing a N-S elongation in emission and a strong emission peak moving away from us. They interpret this in terms of an expanding torus, the axis of which lies along the E-W direction and is normal to the line of sight, with some asymmetry in the CO emission in the torus. Likkel et al. 1989) obtained VLA images at 2 and 6 cm with beam sizes (FWHM) of 0″.5 and 0″.9, respectively, which resolve the nebula. These images show clumpy emission from a slightly elliptical region with full extent of about 4″.5 by 3″.4, with a major axis going from N-NW to S-SE on the sky. Bregman et al. (1992) have obtained a near-infrared K-band image of IRAS 21282+5050 showing a 5″ compact nebula, and detected extended 3 μm PAH emission out to a radius of 20″. These results imply that the PAH molecules exist well beyond the ionized nebula, and Bregman et al. (1992) suggest that they were probably ejected during the preceding AGB phase.

Our high-resolution optical images of IRAS 21282+5050 clearly show it to be extended and elongated along the N-S direction, with a size of 6″.5 × 4″.8. The general elongation direction is similar to that of the CO emission (Shibata et al. 1989), the ionized gas (Likkel et al. 1989), and the dust emission (Bregman et al. 1992) although the radio map shows a slight tilt to the NNW while the optical map shows a slight tilt to NNE.

Our observations, which we interpret as light reflected by the nebula, can be understood in terms of a model with an obscuring torus located perpendicular to the plane of the sky with its axis extending N-S. This would allow the gas to expand preferentially in the polar direction, giving rise to the observed N-S elongated light distribution. The torus, containing obscuring dust, would give rise to much of the large visual extinction found. This interpretation seems to be consistent with the 3.3 μm map of Bregman et al. (1992) as well as with the recent mid-infrared images of IRAS 21282+5050 at the 11.3 μm PAH feature recently obtained by Deutsch et al. (1993) and Meixner et al. (1993). The difference in the orientations between the radio and optical maps can perhaps be explained by the fact that the former represents emission and therefore traces density, whereas the latter represents scattering and fills volume of least extinction.

The CO observations of Shibata et al. (1989) can partly be understood by this model, as it fits with their N-S elongation. However, this model does not naturally explain the high-velocity CO which they detected at the position of the source, and which they interpret as expansion of the far side of the object. If one adopts the model of Shibata et al. (1989) of a torus with its axis of symmetry lying E-W in the plane of the sky, which describes the orientation of the dust as well as the CO, then there is not a simple explanation of why the visible image is elongated N-S. One could perhaps imagine that a torus with its axis lying E-W, but tipped out of the plane of the sky, could reveal a cavity with a N-S elongated cross section from which the scattered visible light and ionized radio emission originate. However, if the dust is oriented with the CO, this removes the dust from the line of sight to the star, and it is this dust which gives rise to the extinction seen. Thus we have not been able to suggest a single model which fits all of these observations.

3.4. *Relationship with Carbon-rich Proto–Planetary Nebulae*

It is interesting to note that recently three carbon-rich proto–planetary nebulae have been suggested to be bipolar based upon their flux distributions (Hrivnak & Kwok 1991). These complement the two well-known bipolar nebulae AFGL 2688 and AFGL 618 in presenting evidence for the development of an asymmetrical shell during the proto–planetary nebula stage. The 3 μm PAH emission features have recently been detected in a few proto–planetary nebulae (Geballe et al. 1992), in particular those with the unidentified 21 μm emission

feature (Kwok, Volk, & Hrivnak 1989) and carbon-rich optical spectra (Hrivnak 1992). These objects possess F-G supergiants as central stars and thus may represent less-evolved analogues to IRAS 21282+5050 and the other carbon-rich WC11 objects discussed here.

While some of the carbon-rich proto–planetary nebulae show features in common with planetary nebulae in the 3 μm region, they also show the presence of a strong 21 μm emission feature not seen in planetary nebulae and the absence of a strong 11.3 μm feature. Since the discovery of the PAH features in NGC 7027, a number (24 out of a sample of 170) of additional planetary nebulae have been found to show the 11.3 μm PAH feature (Volk & Cohen 1990). The difference in the 10–25 μm spectra between these planetary nebulae and the proto–planetary nebulae showing 3 μm features may be due to a change in chemical composition, or a change in the excitation condition of the grain component. It is possible that both the 3 and 21 μm features are due to emission from similarly structured large carbon-based molecules but excited under different radiation environments. The observations of young nebulae like IRAS 21282+5050 will help bridge the gap between proto–planetary nebulae and planetary nebulae.

4. CONCLUSION

In this paper we report optical and infrared photometric measurements of the newly discovered planetary nebula IRAS 21282+5050. As a result we are able to determine its energy distribution, showing it to possess one of the largest infrared excesses observed among planetary nebulae. This suggests that this object has left the AGB only $\sim 10^3$ yr ago.

The weak optical brightness of IRAS 21282+5050, as compared with that in the infrared, suggests that the nebula is heavily obscured by dust. Using a point-source subtraction techinque, we have been able to show that the nebula is extended with a size of $\sim 7'' \times 5''$. This object belongs to the small group of planetary nebulae with WC11 nuclei and 3.3, 7.7, 8.6, 11.3 μm emission features. They are probably related to the newly discovered carbon-rich proto–planetary nebulae with both 3 μm and (unidentified) 21 μm emission features. The study of this group of young planetary nebulae, together with related proto–planetary nebulae, can lead to a further understanding of the chemical evolution of the dust component in post-AGB evolution.

We thank Hugh Harris for obtaining the optical photometry reported in this paper and Lauren Likkel for communicating a map of her radio continuum results before publication. We are also grateful to Rene Racine who helped us in the use of the HRCam on CFHT and Peter Stetson who helped in the analysis of the images. UKIRT is operated by the Royal Observatory of Edinburgh on behalf of the Science and Engineering Research Council. This work is supported by the Natural Sciences and Engineering Research Council of Canada, NASA's Astrophysics Data Program, and by a NASA grant to B. J. H. administered by the American Astronomical Society. B. J. H. also acknowledges the support of a University Research Professorship from Valparaiso University. P. P. L. acknowledges the support of an NSERC postgraduate scholarship.

REFERENCES

Aaquist, O. B., & Kwok, S. 1990, A&AS, 84, 229
———. 1991, ApJ, 378, 599
Aitken, D. K., Barlow, M. J., Roche, P. F., & Spenser, P. M. 1980, MNRAS, 192, 679
Aitken, D. K., & Roche, P. F. 1984, MNRAS, 208, 751
Allen, D. A., Baines, D. W. T., Blades, J. C., & Whittet, D. C. B. 1982, MNRAS, 199, 1017
Balick, B. 1987, AJ, 94, 671
Bregman, J. D., Booth, J., Gilmore, D. K., Kay, L., & Rank, D. 1992, ApJ, 396, 120
Carlson, E. D., & Henize, K. G. 1979, Vistas Astron., 23, 213
Cohen, M., & Jones, B. F. 1987, ApJ, 321, L151
Cohen, M., Tielens, A. G. G. M., & Allamandola, L. J. 1985, ApJ, 299, L93
Cohen, M., Tielens, A. G. G. M., Bregman, J., Witteborn, F. C., Rank, D. M., Allamandola, L. J., Wooden, D. H., & deMuizon, M. 1989, ApJ, 341, 246
Deguchi, S., et al. 1990, ApJ, 351, 522
de Muizon, M., Geballe, T. R., d'Hendercourt, L. B., & Baas, F. 1986, ApJ, 306, L105
Deutsch, L. K., Hora, J. L., Hoffmann, W. F., & Fazio, G. G. 1993, in IAU Symp. 155, Planetary Nebulae, ed. R. Weinberger & A. Acker (Dordrecht: Kluwer), in press
FitzGerald, M. P. 1968, AJ, 23, 983
Geballe, T. R., Tielens, A. G. G. M., Kwok, S., & Hrivnak, B. J. 1992, ApJ, 387, L89
Geballe, T. R., & van der Veen, W. E. C. J. 1990, A&A, 235, L9
Goodrich, R. W., & Dahari, O. 1985, ApJ, 289, 342
Hrivnak, B. J. 1992, in preparation
Hrivnak, B. J., & Kwok, S. 1991, ApJ, 368, 564
Hu, J. Y., & Bibo, E. A. 1990, A&A, 234, 435
Huggins, P. J., & Healy, A. P. 1989, ApJ, 346, 201
IRAS LRS Atlas: Low Resolution Spectra Atlas. 1986, ed. F. M. Olnon & E. Raymond, A&AS, 65, 607
Jourdain de Muizon, M., Cox, P., & Lequeux, J. 1990a, A&AS, 83, 337
Jourdain de Muizon, M., d'Hendercourt, L. B., & Geballe, T. R. 1990b, A&A, 235, 367
Kwok, S. 1990, MNRAS, 244, 179
Kwok, S., Volk, K., & Hrivnak, B. J. 1989, ApJ, 345, L51
Le Bertre, T., Epchtein, N., Gouiffes, C., Heydari-Malayeri, M., & Perrier, C. 1989, A&A, 225, 417
Likkel, L., Forveille, T., Omont, A., & Morris, M. 1988, A&A, 198, L1
———. 1991, A&A, 246, 153
Likkel, L., Morris, M., Omont, A., & Forveille, T. 1989, in IAU Colloq. 106, Evolution of Peculiar Red Giant Stars, ed. H. R. Johnson & B. Zuckerman (Cambridge: Cambridge Univ. Press), 233
Loup, C., Forveille, T., Nyman, L. A., & Omont, A. 1990, A&A, 227, L29
McClure, R., et al. 1989, PASP, 101, 1156
Meixner, M., Ball, J. R., Arens, J. F., & Jernigan, J. G. 1993, in IAU Symp. 155, Planetary Nebulae, ed. R. Weinberger & A. Acker (Dordrecht: Kluwer), in press
Menzies, J. W., & Wolstencroft, R. D. 1990, MNRAS, 247, 177
Nagata, T., Tokynaga, A. T., Sellgren, K., Smith, R. G., Onaka, T., Nakado, Y., & Sakata, A. 1988, ApJ, 326, 157
Neckel, Th., & Klare, G. 1980, ARAS, 42, 251
Roche, P. F., Allen, D. A., & Bailey, J. A. 1986, MNRAS, 220, 7P
Roche, P. F., Aitken, D. K., & Smith, C. H. 1991, MNRAS, 252, 282
Russell, R. W., Soifer, B. T., & Willner, S. P. 1977, ApJ, 217, L149
Shibata, K. M., Tamura, S., Deguchi, S., Hirano, N., Kameya, O., & Tasuga, T. 1989, ApJ, 345, L55
Stetson, P. B. 1987, PASP, 99, 191
van der Hucht, K. A., Conti, P. S., Lundstrom, I., & Stenholm, B. 1981, Space Sci. Rev., 28, 227
van der Veen, W. E. C. J. 1988, Ph.D. thesis, Univ. Leiden
Volk, K., & Cohen, M. 1989, AJ, 98, 931
———. 1990, AJ, 100, 485
———. 1992, ApJS, 80, 347
Volk, K., Kwok, S., & Woodsworth, A. W. 1993, ApJ, 402, 292
Volk, K., & Leahy, D. A. 1993, in IAU Symp 155, Planetary Nebulae, ed. R. Weinberger & A. Acker (Dordrecht: Kluwer), in press
Webster, B. L., & Glass, I. S. 1974, MNRAS, 166, 491
Willner, S. P. 1984, in Galactic and Extragalactic Infrared Spectroscopy, ed. M. F. Kessler & J. P. Phillips (Dordrecht: Reidel), 37
Witteborn, F. C., Sandford, S. A., Bregman, J. D., Allamandola, L. J., Cohen, M., Wooden, D. H., & Graps, A. L. 1989, ApJ, 341, 270
Zhang, C. Y., & Kwok, S. 1991, A&A, 250, 179
Zijlstra, A. A., Gaylard, M. J., te Lintel Hekkert, P., Menzies, J., Nyman, L.-Å., & Schwarz, H. E. 1991, A&A, 243, L9